Thermodynamics of Mesoscopic Vortex Systems in 1 + 1 Dimensions

Chen Zeng,[1] P. L. Leath,[1] and Terence Hwa[2,*]

[1]*Department of Physics and Astronomy, Rutgers University,
Piscataway, New Jersey 08854*
[2]*Center for Study in Physics and Biology, Rockefeller University,
New York, New York 10021*

The thermodynamics of a disordered planar vortex array is studied numerically using a new polynomial algorithm which circumvents slow glassy dynamics. Close to the glass transition, the anomalous vortex displacement is found to agree well with the prediction of the renormalization-group theory. Interesting behaviors such as the universal statistics of magnetic susceptibility variations are observed in both the dense and dilute regimes of this mesoscopic vortex system.

The behavior of vortices in dirty type-II superconductors has been a subject of intense studies in the past decade [1]. Aside from the obvious technological significance of vortex pinning, understanding the physics of such interacting many-body systems in the presence of quenched disorder is a central theme of modern condensed matter physics. Similarities between the randomly pinned vortex system and the more familiar mesoscopic electronic systems [2] are highlighted by a recent experimental study of a planar vortex array threaded through a thin crystal of 2H-NbSe$_2$ by Bolle *et al.* [3]. Interesting behaviors, including the sample-dependent magnetic responses known as "fingerprints," have been observed for such a mesoscopic vortex system.

The disordered planar vortex array is well studied theoretically [4–9]. It is one of the few disorder-dominated systems for which quantitative predictions can be made, including a finite-temperature "vortex glass" phase [5] characterized by anomalous vortex displacements [4], and universal variation of magnetic susceptibility [9]. However, until the work of Bolle *et al.,* there were hardly any experimental studies of this system, with difficulties stemming partly from the weak magnetic signals in such 2D systems. Also, numerical simulations have been limited by the slow glassy dynamics [10], although the availability of special optimization algorithms did lead to the elucidation of the zero-temperature problem in recent years [11]. In this Letter, we describe numerical studies of the thermodynamics of the vortex glass via a mapping to a discrete dimer model with quenched disorder. A new polynomial algorithm for the dimer problem circumvents the glassy dynamics and enables us to study large systems at finite temperatures. Our results obtained in the dilute (single-flux-pinning) regime compare well with the experiment by Bolle *et al.* [3], while those obtained in the collective-pinning regime strongly support the renormalization-group theory of the vortex glass, including its prediction of universal susceptibility variation [9].

The model.— The dimer model consists of all complete dimer coverings $\{D\}$ on a square lattice $\mathcal{L}$ as illustrated in Fig. 1(a). The partition function is

$$Z = \sum_{\{D\}} \exp\left[- \sum_{\langle ij \rangle \in D} \epsilon_{ij}/T_d \right], \qquad (1)$$

where the sum in the exponential is over all dimers of a given covering, and T_d is the dimer temperature. Quenched disorder is introduced via random bond energies ϵ_{ij}, chosen independently and uniformly in the interval $(-\frac{1}{2}, \frac{1}{2})$.

The dimer model is related to the planar vortex-line array via the well-known mapping to the solid-on-solid (SOS) model (see Figs. 1): Take the centers of the square cells of $\mathcal{L}$ to form the dual square lattice $\widehat{\mathcal{L}}$. Orient all bonds of $\widehat{\mathcal{L}}$ such that the elementary squares of $\widehat{\mathcal{L}}$ that enclose the sites of the chosen sublattice of $\mathcal{L}$ [indicated by the solid dots in Fig. 1(a)] are circled counterclockwise. It is now possible to assign a single-valued "height" function $h(\mathbf{r})$ on the lattice points $\mathbf{r}$ of $\widehat{\mathcal{L}}$, such that the difference of every pair of neighboring heights across the oriented bonds is -3 if a dimer is crossed and $+1$ otherwise. For the dimer covering of Fig. 1(a), the values of the associated height function are shown at their respective positions. In terms of the height configuration $h(\mathbf{r})$, the partition function (1) can be written alternatively as $Z = \sum_{\{h(\mathbf{r})\}} e^{-\beta \mathcal{H}[h]}$, where the SOS Hamiltonian takes the
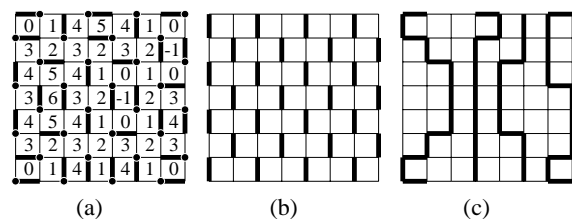

FIG. 1. (a) Snapshot of a dimer covering (thick bonds) together with the associated "height" values $h(\mathbf{r})$ for a lattice of size $L = 8$ at temperature $T_d = 1.0$. (b) Dimer covering of the fixed reference. (c) Vortex-line configuration (thick lines) obtained as the difference between (a) and (b).

following form in the continuum limit:

$$\beta \mathcal{H} = \int d^2 \mathbf{r} \left[\frac{K}{2} (\nabla h)^2 - \mathbf{f}(\mathbf{r}) \cdot \nabla h + g \cos(Gh) \right].$$

$$(2)$$

Here, K is an effective stiffness caused by the inability of a tilted surface to take as much advantage of the low weight bonds as a flatter surface, and $\mathbf{f}(\mathbf{r})$ is a random local tilt bias. The periodicity of the cosine potential in (2) is given by $G = 2\pi/4$ since the smallest "step" of this height profile is four. In the present context of a randomly pinned vortex array, $h(\mathbf{r})$ describes the coarse-grained displacement field of the vortex array with respect to a uniform reference state at the same vortex line density; see Fig. 1(c) and Refs. [5,8]. This mapping between the dimer model and the planar vortex array allows us to compute statistical properties of the vortex array by monitoring appropriate quantities of the dimer model. The latter can be accomplished using a polynomial algorithm described below.

The algorithm.—Computing the partition function of complete dimer coverings on an *arbitrary* weighted lattice is likely to be algorithmically intractable [12]. Weights here refer to the Boltzmann factors $w_{ij} \equiv \exp(-\epsilon_{ij}/T_d)$ on the bonds. A weighted *planar* lattice $\mathcal{G}$ can, however, be *oriented,* denoted by $\vec{\mathcal{G}}$, so that the square root of the determinant of the weighted adjacency matrix defined on $\vec{\mathcal{G}}$ yields the partition function (1) *exactly* [13]. Computation of the determinant can be achieved by various row or column reduction schemes in time that grows *polynomially* with the matrix size.

Recently, Propp and co-workers [14] furnished the above algebraic reduction with an elegant graphical interpretation for the case of bipartite planar lattices [15]. The partition function Z_L on a lattice of linear size L is related to Z_{L-1} as $Z_L(\{w\}) = C(\{w\})Z_{L-1}(\{w'\})$ after a simple weight transformation $\{w\} \to \{w'\}$. The prefactor $C(\{w\})$ is independent of dimer coverings. The partition function is obtained in a "deflation" process in which the above recursive procedure is carried out down to $L = 0$ with $Z_0 = 1$. This deflation process can also be reversed in an "inflation" process where a dimer covering at size $L - 1$ can be used to *stochastically* generate a dimer covering at size L according to Z_L already obtained. Repeating the inflation process thus generates *uncorrelated* "importance samplings" of the dimer configurations, or equivalently the equilibrium height configurations, without the need to run the slow relaxational dynamics. The ensuing numerical results are obtained by taking various measurements of the height configurations generated this way. A somewhat inconvenient feature of this approach is that the algorithm requires an open boundary condition on the dimer model; this in turn fixes the total number of vortex lines, e.g., to $L/2$ on a $L \times L$ lattice (see Fig. 1).

Numerical results.—Since the temperature of the vortex array, given by K^{-1} in (2), is generally different from

the dimer temperature T_d, we first need to calibrate the temperature scale. To do so, we exploit a statistical rotational symmetry [9,16] of the system (2) which guarantees that, at large scales, the effective K is the same as that of the pure system. In particular, K can be obtained by measuring the disorder-averaged thermal fluctuation of the displacement field $\overline{W_T^2} \equiv \overline{\langle \prec h_T^2(\mathbf{r}) \succ \rangle - \langle \prec h_T(\mathbf{r}) \succ^2 \rangle} = (2\pi K)^{-1} \ln(L)$, where $h_T(\mathbf{r}) \equiv h(\mathbf{r}) - \langle h(\mathbf{r}) \rangle$ measures the thermal distortion superposed on the distorted "background" $h_D(\mathbf{r}) \equiv \langle h(\mathbf{r}) \rangle$ by the quenched disorder. We used $\prec \cdots \succ$, $\langle \cdots \rangle$, and overline to denote spatial, thermal, and disorder averages, respectively. With our polynomial algorithm, we were able to perform thorough disorder averages for equilibrated systems of sizes up to 512×512. To reduce boundary effects, we focus on the central $L/2 \times L/2$ piece of the system and compute its displacement fluctuations. Figure 2(a) illustrates the dependence of $\overline{W_T^2}(L)$ for various dimer temperatures T_d. The linear dependence on $\ln(L)$ is apparent. Identifying the proportionality constant with $(2\pi K)^{-1}$, we obtain the empirical relation between K^{-1} and T_d shown in Fig. 2(b). Note that our result recovers the exact relation $K^{-1}(T_d \to \infty) = 16/\pi$ for the dimer model without disorder [17]. Since the glass transition of the system (2) is expected to occur at temperature $K_g^{-1} = 4\pi/G^2 = 16/\pi$, our system is glassy for the entire range of dimer temperatures.

A striking feature of the vortex glass phase is the anomalous fluctuation of the disorder-induced displacement, $\overline{W_D^2} \equiv \overline{\langle \prec h_D^2(\mathbf{r}) \succ \rangle - \langle \prec h_D(\mathbf{r}) \succ^2 \rangle}$. The renormalization group (RG) theory [4] predicts that $\overline{W_D^2}(L) \simeq C_2 \ln^2(L)$ for large L, with the proportionality constant C_2 depending quadratically on the reduced temperature $\tau \equiv K_g/K - 1$ just below the glass-transition temperature K_g^{-1}. We show $\overline{W_D^2}(L)$ vs $\ln(L)$ for different temperatures in Fig. 3(a). The forms of $\overline{W_D^2}(L)$ are well described
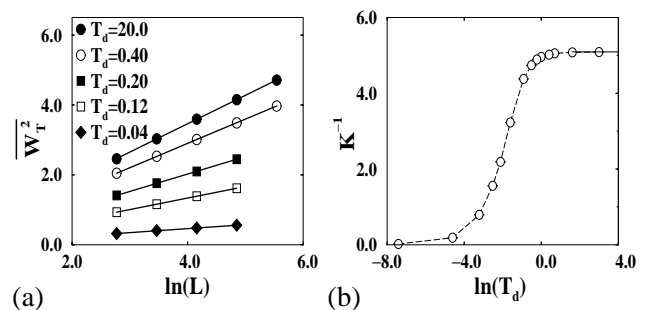

FIG. 2. (a) The disorder-averaged thermal displacement fluctuation $\overline{W_T^2}(L)$ for various dimer temperatures T_d. Each data point was obtained by generating 10^3 thermal samplings for each of 10^3 disorder realizations. The straight lines are fit to $\overline{W_T^2} = (2\pi K)^{-1} \ln(L) + \text{const}$. (b) The extracted relation between K^{-1} and T_d. The horizontal line indicates the asymptotic value of K^{-1} as $T_d \to \infty$.
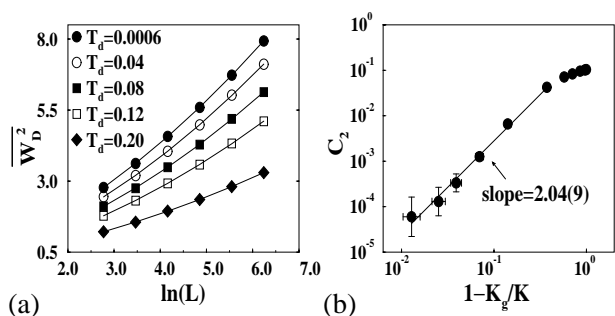
FIG. 3. (a) The anomalous displacement fluctuation $\overline{W_D^2}$ at various dimer temperatures averaged over 10^3 disorder realizations. The lines are fits to the quadratic dependence on $\ln(L)$ expected from the RG theory. (b) Log-log plot of the quadratic coefficient C_2 [extracted from (a)] vs the reduced temperature $\tau = K_g/K - 1$. The best power-law fit yields an exponent of 2.04(9).

FIG. 4. Fractional variance as a function of the reduced temperature, τ, for $L = 32$, 64, 128, and 256 averaged over 10^3 disorder realizations. The solid line is a least-square linear fit for $|\tau| < 0.15$.

by a quadratic function of $\ln(L)$ as predicted. The solid lines are least-square fit to the form $\overline{W_D^2}(L) = C_2 \ln^2(L) + C_1 \ln(L) + C_0$.

To probe the RG prediction further, we examine the temperature dependence of the quadratic coefficient C_2. Plotting C_2 extracted from the quadratic fit in Fig. 3(a) vs the reduced temperature $\tau = K_g/K - 1$ using the vortex temperature K^{-1} obtained in Fig. 2(b) and the exact glass-transition temperature $K_g^{-1} = 16/\pi$, we obtain the data shown in Fig. 3(b). A quadratic dependence of the coefficient C_2 on the reduced temperature τ is clearly demonstrated by the data, thereby providing strong support for the RG theory of the vortex glass.

Another interesting feature of the vortex glass phase is the sample-to-sample variation of the magnetic susceptibility χ. It was predicted [9] that the fractional variance,

$$\text{var}[\chi]/\overline{\chi}^2 \overset{L \to \infty}{\longrightarrow} D|\tau| \qquad \text{for } 0 < -\tau \ll 1, \quad (3)$$

is *universal*, with D being a computable, size-independent constant of order unity. Because of the constraint of fixed vortex density when using the dimer representation, it is not easy to probe the magnetic susceptibility directly by varying vortex density. Instead, we use the fluctuation-dissipation relation, e.g., $\chi \propto \langle(\partial_x h)^2\rangle - \langle \partial_x h \rangle^2$. To circumvent lattice effects, we take as definition $\chi(L) \equiv \mathbf{q}^2(\langle \hat{h}_\mathbf{q} \hat{h}_{-\mathbf{q}} \rangle - \langle \hat{h}_\mathbf{q} \rangle \langle \hat{h}_{-\mathbf{q}} \rangle)$, where $\hat{h}_\mathbf{q}$ is the Fourier transform of $h(\mathbf{r})$, and the right-hand side is evaluated at $(q_x, q_y) = (1/L, 0)$. As shown in Fig. 4, the fractional variance is indeed size independent over the range $L = 32$ to $L = 256$ examined. Its temperature dependence can again be deduced from the relation between K^{-1} and T_d given in Fig. 2(b); it is well described by the linear form (3) close to the glass transition with $D = 0.454(5)$.

The universal variation of magnetic susceptibility is reminiscent of the phenomena of universal conductance fluctuation much studied in mesoscopic electronic systems. This mesoscopic vortex system in fact exhibits interesting
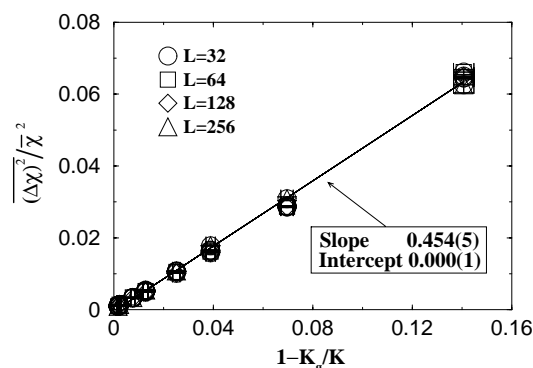
fluctuations even deep into the dilute regime, i.e., close to the threshold field H_{c1}. But, to study the vortex behavior there, we must relax the constraint of fixed vortex number. To do so, we focus on a $L_x \times L_y$ located at the center of the $L \times L$ lattice. Random bond energies are assigned only to this "inner" region. While the total number of vortex lines must be fixed, the number of lines in the inner region can be changed by adding an extra bond energy $\delta\epsilon_{ij} = (-1)^{i+j} v$ in a staggered fashion to all vertical bonds of the staggered reference dimer pattern [Fig. 1(b)] in this region. This has the effect of increasing the "self-energy" of the vortex lines such that when v is sufficiently large, i.e., for $v \geq v_c$, all vortex lines will be *expelled* from the inner region to the outer region; see Fig. 5. A *dilute* regime in the inner region is then achieved for small $\delta v \equiv v_c - v$. This setup could be interpreted as embedding the dirty type-II superconductor of focus within another pure type-II superconductor which has a much smaller H_{c1}. In the limit $L \gg L_x$, the outer region can be regarded as an infinite reservoir in which the vortex density change is negligible. The response we measure will thus come essentially from the inner region.

In Fig. 6(a), we plot the thermal averaged number of vortex lines $\langle n \rangle$ in a thin strip of size $L_x = 16$, $L_y = 256$ embedded in a 512×512 square lattice. We vary the repulsion strength v, holding the temperature fixed at $T_d = 0.01$ (corresponding to only $\sim 10\%$ of the glass
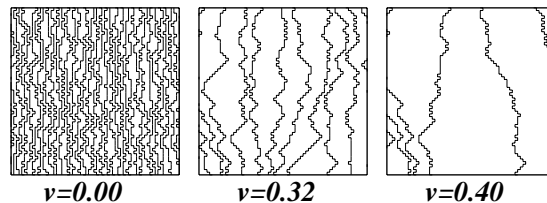

FIG. 5. Snapshots of vortex-line configurations in the inner region at different repulsion strength v for a given disorder realization and $T_d = 0.01$. Quenched disorder exists only in the inner region of size $L_x = L_y = L/2 = 64$.
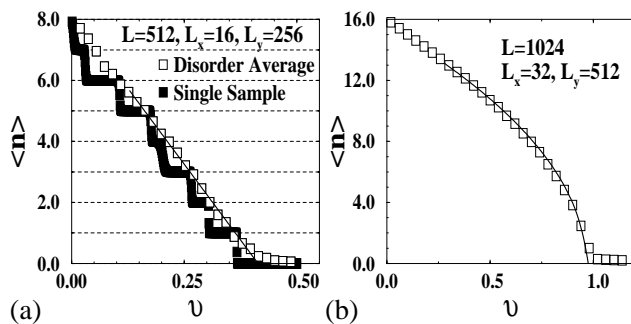
FIG. 6. (a) Average number of vortex lines $\langle n \rangle$ vs different repulsion strength v at temperature $T_d = 0.01$ in a narrow $L_x \times L_y$ stripe. The solid squares are for a given disorder realization and the open squares denote results from average over 100 realizations. The line is a fit to linear dependence in the vicinity of the threshold v_c. Slight rounding near v_c is due to the small but still finite ratio L_x/L. (b) $\langle n \rangle$ vs v in the absence of disorder. The line is a fit to the square-root form expected in the vicinity of v_c.

transition temperature). The solid squares are data taken from a *given* realization of disorder. We see a disordered staircase structure in the dependence of $\langle n \rangle$ on δv, similar to experimental magnetic response curves observed by Bolle *et al.* [3]. The step width dispersion results from a delicate energetic balance between the line-line repulsion and the random pinning; it can be regarded as a *fingerprint* of this disordered sample. By averaging such staircase-response curves over 100 realizations. we obtain results indicated by the open squares in Fig. 6(a). We can extract a linear dependence, i.e., $\overline{\langle n \rangle} \sim \delta v$ (except for finite-size rounding very close to the threshold). This finding agrees well with the experimental result of Bolle *et al.* [3]. It should be contrasted with the very different behavior when the disorder is absent. The latter is shown in Fig. 6(b) for a system which is twice larger in all linear dimensions. The data are well described by a square-root singularity, $\langle n \rangle \sim (\delta v)^{1/2}$, as expected from the theory of Pokrovsky and Talapov [18]. The origin of the anomalous linear dependence of $\overline{\langle n \rangle}$ on δv in the random case has been discussed previously [8,19]; it can be readily understood from the properties of a single vortex line pinned in a two-dimensional random potential.

Conclusion. — Finite-temperature simulations were performed on a disordered dimer model to study various equilibrium properties of a planar array of vortex lines. Numerical results on the anomalous displacement fluctuation strongly support the renormalization-group theory of vortex glass. Universal susceptibility variations in the collective pinning regime were observed in accordance with the theory; critical behaviors near the glass transition compared well with analytic predictions. Suitable modification of the dimer model allowed a direct study of the dilute regime where a few vortex lines penetrate the system. Disordered staircaselike magnetic fingerprints were obtained; the statistics are in agreement with theoretical

predictions, and drastically different from the well-known behavior of the pure system. The numerical findings in the dilute regime are also in agreement with recent experiment on a micron-sized single crystal of 2H-NbSe$_2$. It is hoped that the present study will stimulate further experimental investigations of the fascinating physics of mesoscopic vortex systems.

*Permanent address: Physics Department, University of California at San Diego, La Jolla, CA 92093-0319.
[1] G. Blatter *et al.,* Rev. Mod. Phys. **66**, 1125 (1994).
[2] *Mesoscopic Quantum Physics,* edited by E. Akkermans *et al.* (North-Holland, Amsterdam, 1994).
[3] C. A. Bolle *et al.,* Nature (London) **399**, 43 (1999).
[4] See, e.g., J. L. Cardy and S. Ostlund, Phys. Rev. B **25**, 6899 (1982); J. Toner and D. P. DiVincenzo, Phys. Rev. B **41**, 632 (1990).
[5] M. P. Fisher, Phys. Rev. Lett. **62**, 1415 (1989).
[6] T. Nattermann, I. Lyuksyutov, and M. Schwartz, Europhys. Lett. **16**, 295 (1991).
[7] T. Giamarchi and P. Le Doussal, Phys. Rev. B **52**, 1242 (1995).
[8] T. Hwa, D. R. Nelson, and V. M. Vinokur, Phys. Rev. B **48**, 1167 (1993).
[9] T. Hwa and D. S. Fisher, Phys. Rev. Lett. **72**, 2466 (1994).
[10] G. G. Batrouni and T. Hwa, Phys. Rev. Lett. **72**, 4133 (1994); E. Marinari, R. Monasson, and J. J. Ruiz-Lorenzo, J. Phys. A **28**, 3975 (1995); D. Cule and Y. Shapir, Phys. Rev. Lett. **74**, 114 (1995).
[11] See, e.g., C. Zeng, A. A. Middleton, and Y. Shapir, Phys. Rev. Lett. **77**, 3204 (1996); H. Rieger and U. Blasum, Phys. Rev. B **55**, R7394 (1997).
[12] L. G. Valiant, Theor. Comput. Sci. **8**, 189 (1979).
[13] P. W. Kasteleyn, Physica (Utrecht) **27**, 1209 (1961); M. E. Fisher, J. Math. Phys. **7**, 1776 (1966).
[14] N. Elkies, G. Kuperberg, M. Larsen, and J. Propp, J. Algebr. Comb. **1**, 111 (1992); **1**, 219 (1992); J. Propp, "Urban Renewal," available from http://www.math.wisc.edu/~propp/articles.html
[15] The graphical scheme was described for a square lattice of Aztec diamond shape [14]. This poses no real restriction, however, since any bipartite planar graph can always be embedded in an Aztec diamond of sufficient size in which the dimer covering outside the graph is frozen and makes no contribution to the partition function.
[16] U. Schulz *et al.,* J. Stat. Phys. **51**, 1 (1988).
[17] See, e.g., R. W. Youngblood, D. J. Axe, and B. M. McCoy, Phys. Rev. B **21**, 5212 (1980); C. L. Henley, J. Stat. Phys. **89**, 483 (1997).
[18] V. L. Pokrovsky and A. L. Talapov, Phys. Rev. Lett. **42**, 65 (1979).
[19] M. Kardar, Nucl. Phys. **B2090**, 582 (1987).